THE JOURNAL OF BIOLOGICAL CHEMISTRY VOL. 288, NO. 49, pp. 35237–35252, December 6, 2013

Tyr^{728} in the Kinase Domain of the Murine Kinase Suppressor of RAS 1 Regulates Binding and Activation of the Mitogen-activated Protein Kinase Kinase*

Received for publication, June 4, 2013, and in revised form, October 11, 2013 Published, JBC Papers in Press, October 24, 2013, DOI 10.1074/jbc.M113.490235

Claudia Sibilski[‡], Thomas Mueller[§], Laxmikanth Kollipara[¶1], René P. Zahedi[¶1], Ulf R. Rapp[‡‖], Thomas Rudel[‡2], and Angela Baljuls[‡3]**

*From the [‡]Department of Microbiology, Biocenter, and the [§]Department of Molecular Plant Physiology and Biophysics, Julius-von-Sachs Institute for Biosciences, University of Wuerzburg, 97074 Wuerzburg, Germany, the [¶]Leibniz-Institut für Analytische Wissenschaften, ISAS-e.V., 44139 Dortmund, Germany, the [‖]Division Molecular Mechanisms in Lung Cancer, Max Planck Institute for Heart and Lung Research, 61231 Bad Nauheim, Germany, and **Systems Biology Ireland, Conway Institute, University College Dublin, Dublin 4, Ireland*

Background: KSR1 coordinates the assembly of RAF-MEK-ERK complexes and regulates signal transduction.
Results: LCK-dependent phosphorylation of KSR1 on Tyr^{728} regulates MEK binding and activation.
Conclusion: Tyr^{728} phosphorylation may coordinate the transition between the scaffolding and catalytic function of KSR1 to fine-tune cellular responses.
Significance: Tyrosine phosphorylation of KSR1 is a new regulatory link between Src family kinases and RAF/MEK/ERK signaling.

In metazoans, the highly conserved MAPK signaling pathway regulates cell fate decision. Aberrant activation of this pathway has been implicated in multiple human cancers and some developmental disorders. KSR1 functions as an essential scaffold that binds the individual components of the cascade and coordinates their assembly into multiprotein signaling platforms. The mechanism of KSR1 regulation is highly complex and not completely understood. In this study, we identified Tyr^{728} as a novel regulatory phosphorylation site in KSR1. We show that Tyr^{728} is phosphorylated by LCK, uncovering an additional and unexpected link between Src kinases and MAPK signaling. To understand how phosphorylation of Tyr^{728} may regulate the role of KSR1 in signal transduction, we integrated structural modeling and biochemical studies. We demonstrate that Tyr^{728} is involved in maintaining the conformation of the KSR1 kinase domain required for binding to MEK. It also affects phosphorylation and activation of MEK by RAF kinases and consequently influences cell proliferation. Moreover, our studies suggest that phosphorylation of Tyr^{728} may affect the intrinsic kinase activity of KSR1. Together, we propose that phosphorylation of Tyr^{728} may regulate the transition between the scaffolding and the catalytic function of KSR1 serving as a control point used to fine-tune cellular responses.

KSR (kinase suppressor of RAS) is an essential scaffold protein that coordinates the assembly and localization of the RAF-MEK-ERK complexes and regulates fidelity, intensity, and duration of MAPK signaling (for review see Refs. 1 and 2). Although KSR knock-out mice are developmentally normal, they are less susceptible to RAS-mediated skin cancer (3), which underscores the importance of KSR in the regulation of MAPK-mediated cell proliferation and tumorigenesis. In mammals, the KSR protein family consists of two members, KSR1 and KSR2. The KSR homologs expressed in *Drosophila* and *Caenorhabditis elegans*, and the mammalian KSR proteins share five highly conserved regions (CA1–5) (4–7). KSR family members are structurally related to RAF kinases. The CA3 domain is similar to the cysteine-rich domain of RAF and is required for membrane recruitment of KSR. CA4 is a serine/threonine-rich region similar to CR2 (conserved region 2) of RAF, whereas CA5 is highly homologous to the kinase domain (CR3) of RAF proteins (1). Although KSR members contain a kinase domain, the issue, whether mammalian KSR has kinase activity or is a pseudokinase, is controversially discussed (8–13). The main argument for mammalian KSR being a pseudokinase is the substitution of a lysine residue in subdomain II of the KSR kinase domain, which is highly conserved in RAF and other kinases and is considered essential for catalytic activity because of a coordination function in ATP binding (4, 5, 14). Interestingly, *C. elegans* KSR1 and *Drosophila* KSR contain the invariant lysine in subdomain II, which would suggest that they are catalytically competent (2). However, mutation of the invariant lysine residue in *Drosophila* KSR does not compromise its function, suggesting either that KSR proteins do not require catalytic activity to maintain their functionality or that

* This work was supported by Deutsche Forschungsgemeinschaft Grant SFB 487, under Project C3 (to U. R. R.) and Project B2 (to T. M.), by University of Wuerzburg Fellowship "Chancengleichheit für Frauen in Forschung und Lehre" (to C. S.), by a Deutsche Forschungsgemeinschaft Fellowship (to A. B.), and by the Science Foundation Ireland under Grant 06/CE/B1129.
[1] Supported by the Ministerium für Innovation, Wissenschaft und Forschung des Landes Nordrhein-Westfalen.
[2] To whom correspondence may be addressed: Department of Microbiology, Biocenter, University of Wuerzburg, Am Hubland, 97074 Wuerzburg, Germany. Tel.: 49-931-31-84401; Fax: 49-931-31-84402; E-mail: thomas.rudel@biozentrum.uni-wuerzburg.de.
[3] To whom correspondence may be addressed: Systems Biology Ireland, Conway Institute, University College Dublin, Belfield, Dublin 4, Ireland. Tel.: 353-1-7166979; E-mail: angela.baljuls@ucd.ie.

the catalytic competence of KSR (in contrast to other kinases) does not absolutely require a lysine residue in this position (15).

KSR has been shown to associate with RAF, MEK, and ERK and to promote the formation of large molecular weight complexes for facilitating signal transduction (10, 16). MEK is constitutively associated with KSR, whereas RAF and ERK bind only in response to a stimulus (1, 17). ERK binds to the CA4 of KSR that includes a F*X*FP motif. This motif is also known as the DEF (docking site for ERK) domain (18, 19). The interaction with MEK is mediated by the CA5 of KSR. The recently published structure of the kinase domain of KSR2 in complex with MEK1 revealed that interaction between KSR and MEK occurs in a face to face manner involving their respective activation segments and αG helices, whereas association of KSR with RAF utilizes the side to side dimerization interface (13, 20).

Regulation of the KSR scaffolding property is complex and, to date, not fully understood. Numerous factors, including binding to 14-3-3, heat shock proteins 70 and 90, cdc37 and G-protein γ subunit, phosphorylation by PKA, C-TAK1, and ERK, and dephosphorylation by PP2A have been reported to regulate KSR functions (10, 17, 21–25). The binding of heat shock proteins and cdc37 to KSR is required for protein stability, because pharmacologically induced disruption of these interactions results in rapid KSR degradation (10). 14-3-3 binding regulates the recruitment of KSR to the plasma membrane and stabilizes the inactive and active conformations of KSR (17, 21). The recruitment of KSR to membrane compartments is a dynamic process that depends on C-TAK1-mediated phosphorylation and PP2A-dependent dephosphorylation of 14-3-3 binding sites located on either side of the CA3 domain in KSR (24, 25). The feedback phosphorylation by ERK promotes KSR1/B-RAF dissociation and the release of KSR1 from the plasma membrane (17, 26, 27).

Tyrosine kinases of the Src protein family are important regulators of the MAPK signal transduction pathway. It has been shown that Src activity is required for rapid activation of ERK signaling (28) and that Src kinases can phosphorylate several proteins of the cascade including EGFR, RAS-GAP, and RAF (29–34). However, studies of mouse cells lacking three members of the Src family (Src, Yes, and Fyn) indicate that Src kinases are mostly dispensable for receptor tyrosine kinase signaling (35). Thus, the interplay between Src kinases and MAPK signaling is complex. In an effort to identify a new regulatory link between Src kinases and MAPK signal transduction, we have searched for potential tyrosine phosphorylation site(s) in KSR1. Mass spectrometry analysis of mouse KSR1 coexpressed with LCK (the lymphocyte-specific member of the Src family) identified Tyr^{728} as a novel phosphorylation site. The LCK-mediated phosphorylation of Tyr^{728} was confirmed by substitution with nonphosphorylatable phenylalanine. To determine the role of Tyr^{728} phosphorylation in the regulation of KSR1 *in vivo*, we investigated the effect of Tyr^{728} substitution on KSR1/MEK interaction, MEK activation, and cell proliferation. The *in vivo* studies were accomplished by *in silico* analysis of a KSR1 homology model structure and molecular dynamics simulations thereof. Here, we show that the amino acid at position 728 has a dual importance for the functional properties of KSR1. First, it is involved in maintaining the "bound" conformation of KSR1 kinase domain in complex with MEK and therefore influences KSR1/MEK association. Second, it affects phosphorylation of MEK by RAF and consequently influences cell proliferation. Moreover, our *in silico* studies suggest that phosphorylation of Tyr^{728} may affect the intrinsic kinase activity of KSR1. In conclusion, phosphorylation of Tyr^{728} may regulate the transition between the scaffolding and the catalytic function of KSR1 serving as a control point used to fine-tune cellular responses.

EXPERIMENTAL PROCEDURES

Cell Lines, Plasmids, and Antibodies—Immortalized KSR1$^{-/-}$ mouse embryonic fibroblasts (MEFs)[4] and retroviral vectors (empty and KSR1-carrying MSCV-IRES-GFP, as well as an ecotropic packaging vector) were kindly provided by the group of Robert E. Lewis (University of Nebraska Medical Center, Omaha, NE). Anti-LCK (sc-433), anti-MEK1 (sc-219), anti-B-RAF (sc-166), anti-GFP (sc-9996), and anti-actin (sc-1616) antibodies were obtained from Santa Cruz Biotechnology. Anti-phospho-MEK1/2 (9121) antibody was from Cell Signaling Technology. Anti-GST (A5800) antibody was purchased from Invitrogen. Anti-KSR1 (611576) was from BD Biosciences. Anti-Tyr(P) (clone 4G10) antibody was produced in house.

Cloning of GST-tagged KSR1 Wild Type and Mutants—Murine KSR1 cDNA was amplified by PCR. The upstream primer sequence was 5′-GGACTAGTATGGATAGAGCGGCGTTGCG-3′, which contained a SpeI restriction site (underlined). The downstream primer sequence with a NotI restriction site (underlined) was 5′-ATTTGCGGCCGCCTAATGGTGATGGTGATGGTG-3′. KSR1 cDNA and the mammalian expression vector pEBG were cut with SpeI and NotI enzymes and subsequently ligated by use of T4 DNA ligase to give the expression plasmid for N-terminal GST-tagged and C-terminal His-tagged murine KSR1. The *Pfu* DNA polymerase was purchased from Agilent Technologies. Restriction enzymes and T4 DNA ligase were obtained from Thermo Scientific.

The site-specific mutations in the kinase domain of KSR1 were introduced using a QuikChange site-directed mutagenesis kit (Agilent Technologies) according to the manufacturer's instructions. Mutations were verified by DNA sequencing.

Cell Culture and Transfection—COS7 and 293T cells were grown in DMEM (Sigma) containing 10% FBS (PAA Laboratories) and 2% penicillin/streptomycin (Invitrogen). KSR1$^{-/-}$ MEFs were cultivated in DMEM supplemented with 10% FBS, 1% penicillin/streptomycin, and 0.1 mM minimum essential medium with non-essential amino acids (minimum Eagle's medium with non-essential amino acids; Invitrogen). COS7 cells were transiently transfected with a total of 8 μg of recombinant DNA/10-cm dish using jetPEI transfection reagent (Polysciences, Inc.) according to the manufacturer's instructions.

Generating of Stable Cell Lines—KSR1 retroviruses were generated by cotransfecting KSR1-carrying MSCV-IRES-GFP retroviral expression plasmids with an ecotropic packaging vector into 293T cells. Viral supernatants were then used to infect

[4] The abbreviations used are: MEF, mouse embryonic fibroblast; MD, molecular dynamics; r.m.s., root mean square; KD, kinase domain.

KSR1$^{-/-}$ MEFs in the presence of 6 μg/ml polybrene. Control cells were infected with retroviruses carrying empty vector (MSCV-IRES-GFP). Pools of GFP-expressing MEFs were sorted by FACS according to increasing levels of fluorescence. For measuring the base-line fluorescence, uninfected cells were used. Expression of KSR1 was proportional to the GFP expression level. KSR1 and GFP expression was confirmed by SDS-PAGE and Western blot analysis.

Proliferation Assay—To synchronize the cell cycle, MEFs were starved for 24 h in medium containing 0.5% FBS. After synchronization, MEFs were seeded in triplicate 6-well plates (3×10^4 cells/well) and cultivated in medium containing 10% FBS for 3 days. To keep the cells in the exponential growth phase over the time frame of the assay, MEFs were trypsinized, counted by FACS, and seeded again (2×10^4 cells/well). The procedure was repeated three more times, and the assay was stopped on day 12 after the first seeding.

Coprecipitation Assay—24 h post-transfection, cells were lysed with coprecipitation buffer containing 10 mM Tris-HCl (pH 8.0), 50 mM sodium chloride, 30 mM sodium pyrophosphate, 1 mM sodium orthovanadate, 1% (v/v) Nonidet P-40 (Nonidet P-40), and a mixture of protease inhibitors (Roche) for 1 h with gentle rotation at 4 °C. All lysates were clarified by centrifugation at 16,100 $\times$ *g* for 15 min at 4 °C. GST-tagged KSR1 was precipitated by incubating the supernatants with 80 μl of glutathione-Sepharose beads (GE Healthcare) for 3–4 h at 4 °C with rotation. After incubation, the beads were washed three times with coprecipitation buffer containing 0.1% (v/v) Nonidet P-40, supplemented with Laemmli buffer, and boiled for 5 min at 100 °C.

Isolation of GST-fused KSR1 for MS Analysis—For preparation of recombinant KSR1 protein, COS7 cells were seeded in 25 10-cm dishes and transfected with 6 μg of KSR1 and 2 μg of kinase-active LCK-Y505F. 24 h post-transfection, cells were washed once with PBS followed by lysis with buffer containing 25 mM Tris-HCl (pH 7.6), 150 mM sodium chloride, 25 mM β-glycerophosphate, 25 mM sodium fluoride, 10 mM sodium pyrophosphate, 10 mM β-mercaptoethanol, 1 mM sodium orthovanadate, 10% (v/v) glycerol, 0.75% (v/v) Nonidet P-40, and standard proteinase inhibitors for 1 h with gentle rotation at 4 °C. The lysates were clarified by centrifugation at 16,100 $\times$ *g* for 15 min at 4 °C. The supernatant containing GST-tagged KSR1 protein was incubated with 1 ml of glutathione-Sepharose beads for 2 h at 4 °C with rotation. After incubation, the beads were washed three times with buffer containing 25 mM Tris-HCl (pH 7.6), 300 mM sodium chloride, 25 mM β-glycerophosphate, 25 mM sodium fluoride, 10 mM sodium pyrophosphate, 10 mM β-mercaptoethanol, 1 mM sodium orthovanadate, 10% (v/v) glycerol, 0.2% (v/v) Nonidet P-40, and standard proteinase inhibitors. Beads were poured into a column, and GST-KSR1 was eluted with 3 ml of buffer containing 50 mM Tris-HCl (pH 8.0), 20 mM glutathione, 1 mM sodium orthovanadate, and standard proteinase inhibitors by collecting several fractions. The purity of recombinant KSR1 was documented by SDS-PAGE, Western blot analysis, and staining with Coomassie Blue.

In-gel Digestion for MS Analysis—Approximately 2 μg of each sample were separated by SDS-PAGE. Proteins were then visualized by silver staining, and digestion of excised gel slices was done as described previously (36).

In-solution Digestion for MS—In-solution digestion was performed according to Burkhart *et al.* (37). Briefly, an aliquot of each sample corresponding to ~20 μg of protein was diluted to 200 μl with 50 mM ammonium bicarbonate. Disulfide bonds were reduced using 10 mM DTT for 30 min at 56 °C, and free thiols were subsequently alkylated with 30 mM iodoacetamide for 30 min at room temperature in the dark. Trypsin (Promega) was added in a 1:25 (w/w) enzyme to substrate ratio, and samples were incubated overnight at 37 °C. Alternatively, samples were digested with 1:20 (w/w) Pronase E (*Streptomyces griseus*; Sigma-Aldrich) for 1 h at 40 °C, in the presence of phosSTOP (Roche Diagnostics). Digestion efficiency was monitored as described previously (37).

Enrichment of Phosphopeptides—Peptides generated from both enzymatic digestions were acidified with 2% TFA and desalted using C18 solid phase extraction tips (OMIX; Agilent Technologies) according to the manufacturer's instructions. Subsequently, titanium dioxide-based phosphopeptide enrichment was conducted as described previously (38). All obtained eluates were analyzed using LC-MS/MS.

LC-MS/MS Analysis—Samples were analyzed on LTQ-Orbitrap XL or LTQ-Orbitrap Velos mass spectrometers (Thermo Scientific), both online coupled to Ultimate 3000 RSLC systems (Thermo Scientific). Peptides were loaded in 0.1% TFA on a C18 trapping column (Acclaim Pepmap RSLC, 100 μm $\times$ 2 cm; Thermo Scientific) and separated on a C18 main column (Acclaim Pepmap RSLC, 75 μm $\times$ 15 cm) using a binary gradient (A: 0.1% formic acid; B: 0.1% formic acid, 84% acetonitrile) ranging from 5 to 50% B in 49 min, at a flow rate of 300 nl/min. Dedicated wash blanks were introduced between consecutive samples to eliminate memory effects (39). MS survey scans were acquired in the Orbitrap from m/z 300 to 2000 at a resolution of 60,000 using the polysiloxane m/z 445.120030 as lock mass (40). The five most intense signals were subjected to collision-induced dissociation in the ion trap, using multistage activation and taking into account a dynamic exclusion of 30 s. Collision-induced dissociation spectra were acquired with a normalized CE of 35%, an isolation width of 2 m/z, an activation time of 30 ms, and a maximum injection time of 100 ms. For multistage activation, neutral losses of phosphoric acid and water were considered. Automatic gain control target values were set to 10^6 for MS and 10^4 for MS/MS scans.

MS Data Processing and Interpretation—Raw MS data were converted into mgf format using the ProteoWizard software 2.2.0 (41). Obtained peak lists were searched against a concatenated target/decoy version of the UniProt mouse database, including isoforms, using Mascot 2.4 (Matrix Science), OMSSA 2.1.9, and X!Tandem (version 01.01.2010) with the help of searchGUI 1.10.4 (42). Trypsin with a maximum of two missed cleavages was selected as enzyme, whereas no enzyme was chosen for Pronase E samples. Phosphorylation of Ser/Thr/Tyr was selected as variable modification. MS and MS/MS tolerances were set to 10 ppm and 0.4 Da, respectively. Finally, validation of identified peptides and phosphopeptides was done using the PeptideShaker software 0.18.3, applying a false discovery rate of 1% at the peptide-spectrum-match level. Only phosphorylation

site localizations meeting the following criteria were considered as confident: (i) the number of phosphorylations equals the number of potential phosphorylation sites, (ii) the peptide is singly phosphorylated and passed a 1% false localization rate threshold, or (iii) the peptide is multiply phosphorylated and has a D-score of >95% (43)

Modeling of the Three-dimensional Structure of the Mouse KSR1 Kinase Domain—The model of the mouse KSR1 kinase domain (UniProt identifier Q61097, residues Ser^{550} to Leu^{830}) was built on the basis of the template structure of human KSR2 in complex with MEK1 (Protein Data Bank entry 2Y4I) (13). Sequence alignment between the target KSR1 and the template yielded an amino acid sequence identity of 69% and a homology of almost 86% over 280 residues. For modeling the KSR2 chain was stripped from the MEK1 molecule present in the structure of the complex, and differing amino acid residues were exchanged to those present in mouse KSR1 using the ProteinDesign tool in the software package Quanta2008 (MSI Accelrys, San Diego, CA). Two substitutions involved an exchange from another amino acid to a proline residue or vice versa. For all amino acid replacements, rotamer searches were performed to minimize steric constraints before fitting in the side chain. A short energy minimization (50 steps of conjugate gradient minimization, all-hydrogen force field Charmm27; MSI Accelrys) using only geometrical energy terms with the backbone restrained with strong harmonic potential (energy constant 50 kcal mol^{-1} Å^{-2}) was performed to allow bonds and angles of substituted residues to be relaxed. Finally, all exchanges could be performed without causing bad van der Waals contacts in the final structure of mouse KSR1. The interaction of KSR2 with MEK1 occurs mainly by facing their catalytic sites, implicating activation segment and αG helix, respectively, each other (13).

Molecular Dynamics (MD) Simulations of KSR1 Kinase Domain—To test the influence of the phosphorylation onto the structure of KSR1 kinase domain, MD simulations in explicit water were performed using the software package NAMD/visual molecular dynamics (version 2.9). The model structures of the Tyr^{728}-phosphorylated and nonphosphorylated mouse KSR1 variants were first energy minimized in Quanta2008 (MSI Accelrys) to remove possible bad van der Waals contacts using only geometrical energy terms employing 500 steps conjugate gradient minimization and the Charmm27 all-hydrogen force field. Then the model structures were placed into a rectangular water box (TIP3 water) to cover the protein with an at least 25-Å-thick solvent layer yielding a final box with dimensions 93 × 92 × 100Å. The overall charge of the box containing protein and solvent was then first neutralized by the module autoionize 1.3 and then to add additional 150 mM potassium chloride. For the KSR1 model with Tyr(P)^{728}, the box contained, in addition to the protein molecule (residues Ser^{550}–Leu^{830}), 25,344 TIP3 water molecules, 72 chloride ions, 76 potassium ions, 1 magnesium ion, and 1 ATP molecule. For the KSR1 model with nonphosphorylated Tyr^{728}, the same procedure was applied. For simulations, the Charmm27 all-hydrogen force field was used, periodic boundaries were set to the above described box dimensions, and the particle mesh Ewald method was applied to the box to treat electrostatic interactions. A cutoff of 12 Å was chosen for van der Waals and electrostatic interactions with a switching function starting at a distance of 10 Å. All simulations were performed as Langevin dynamics at a temperature of 310 K, a damping coefficient of 1 ps^{-1} and constant pressure of 1.01325 bars with a time step of 1 (or 2 for final minimization and production) fs. Bonds involving hydrogens were kept rigid by applying the SHAKE algorithm. The system KSR1-Tyr(P)^{728} containing 80,780 atoms in total (KSR1-Tyr^{728}: 80,773 atoms) was then equilibrated in a stepwise procedure. First a 0.5-ns trajectory with all protein heavy atoms including the ATP molecule and the magnesium ion kept fixed was performed to allow for minimization of the hydrogens, the solvent molecules as well as the ions to allow for proper distribution of the ions within the box. Then protein and ATP atoms were stepwise released, first with a short 0.1-ns trajectory and a harmonic potential on protein/ATP heavy atoms of 20 kcal mol^{-1} Å^{-2}, then another 0.1-ns simulation by employing 4 kcal mol^{-1} Å^{-2} harmonic restraints, and then a final 0.5-ns minimization with no restraints. Then a production trajectory was calculated with 5-ns duration (2-fs time steps). The final 5-ns trajectories were analyzed in visual molecular dynamics with respect to hydrogen bond formation and root mean square (r.m.s.) deviation of various secondary structure and loop elements.

RESULTS

LCK Interacts with KSR1 for Tyrosine Phosphorylation—In its amino acid sequence and pattern of regulation, KSR1 shows a high homology to RAF kinases, which are known to be regulated by Src family kinases (32, 33). Therefore, we hypothesized that KSR1 may also be phosphorylated and regulated by tyrosine kinases of the Src protein family. To test this assumption, we coexpressed GST-fused murine KSR1 with active (Y505F) or inactive (K273E/Y505F) LCK mutants in COS7 cells and precipitated KSR1 with glutathione-Sepharose beads. As shown in Fig. 1*A*, KSR1 coexpressed with the active LCK was tyrosine-phosphorylated. In contrast, no tyrosine phosphorylation was found in the KSR1 sample coexpressed with kinase-inactive LCK, suggesting that LCK binds and phosphorylates KSR1 on as yet unknown tyrosine residue(s). These results were confirmed by use of LCK inhibitor III (428207; Calbiochem). Treatment of cells with the inhibitor completely abolished the LCK-induced tyrosine phosphorylation of KSR1 (Fig. 1*B*).

MS Analysis of KSR1 Identified Tyr^{728} *as a Target for LCK-mediated Phosphorylation*—We next searched for candidate tyrosine residues in KSR1 that can be phosphorylated by Src family kinases. *PhosphoSitePlus* (a database of observed post-translational protein modifications) refers Tyr^{673} of mouse KSR1 as a potential phosphorylation site identified by MS analysis. To prove whether Tyr^{673} is a target for LCK-mediated phosphorylation and to identify further candidate tyrosine residue(s), which might be phosphorylated by LCK, we performed MS analysis of GST-KSR1 coexpressed with active LCK-Y505F mutant in COS7 cells and purified by binding to glutathione-Sepharose. Three independent MS measurements provided up to 78% coverage of the entire protein sequence. The combined results obtained for murine KSR1 phosphorylation are summarized in Fig. 2*A*. In addition to several serine and threonine

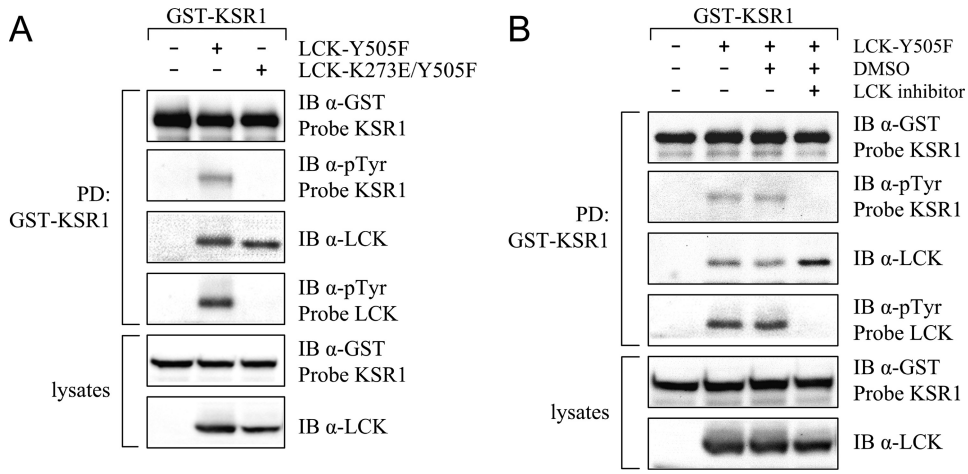

FIGURE 1. **LCK binds to KSR1 and phosphorylates it on tyrosine residue(s).** *A*, kinase-active (Y505F) and kinase-inactive (K273E/Y505F) LCK were coexpressed with GST-KSR1 in COS7 cells. Phosphorylation levels of precipitated GST-KSR1 and KSR1-bound LCK were detected by use of an anti-phosphotyrosine antibody. *B*, COS7 cells were transfected with LCK-Y505F and GST-KSR1 and treated with LCK inhibitor III (100 μM) or solvent (dimethyl sulfoxide, *DMSO*) for 2 h prior to cell harvesting. GST-KSR1 was precipitated and tested for binding of LCK and tyrosine phosphorylation. *PD*, pulldown; *IB*, immunoblot; α, anti.

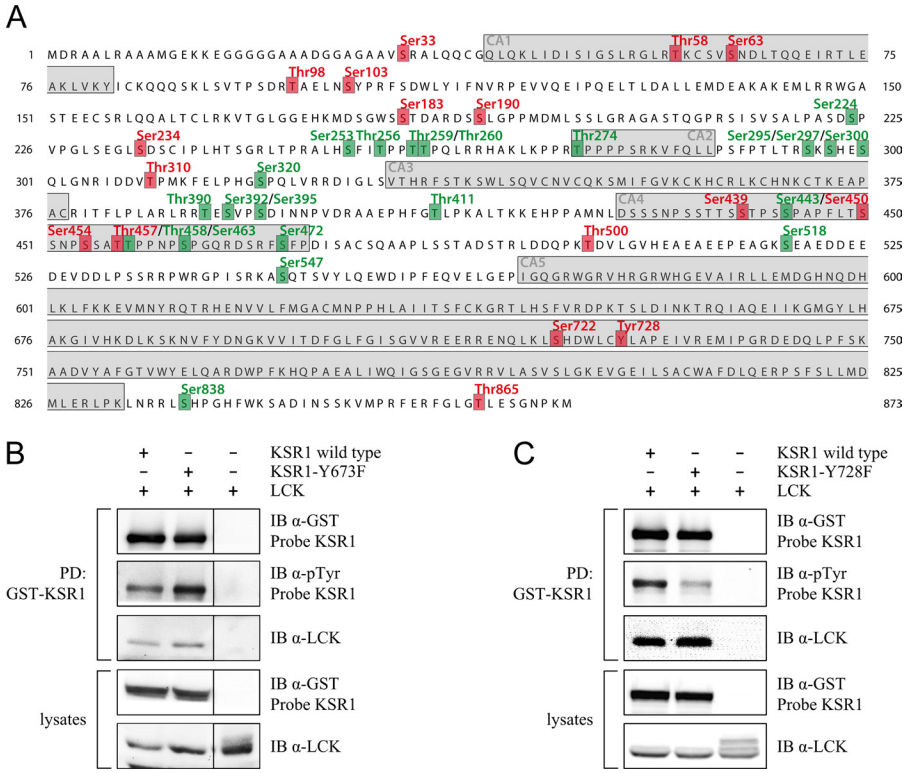

FIGURE 2. **LCK phosphorylates KSR1 on Tyr^{728}.** *A*, amino acid sequence of the murine KSR1 depicting phosphorylation sites identified by MS analysis. The known phosphorylation sites are highlighted in *green*, whereas the newly identified confident phosphorylation sites are highlighted in *red*. The conserved regulatory domains are *shaded* in *gray*. *B* and *C*, GST-tagged KSR1 WT and mutants Y673F (*B*) and Y728F (*C*) were coexpressed with active LCK in COS7 cells and precipitated by use of glutathione-Sepharose beads. The levels of tyrosine phosphorylation were detected by an anti-phosphotyrosine antibody. *PD*, pulldown; *IB*, immunoblot; α, anti.

residues known for phosphorylation in KSR1, we could identify 17 so far unknown confident phosphorylation sites. Intriguingly, one of the newly identified phosphorylation sites was Tyr^{728}, which was detected only in the KSR1 sample coexpressed with LCK, suggesting that this tyrosine is phosphorylated by LCK. However, our MS analysis did not confirm phosphorylation of Tyr^{673}.

Next, we mutated Tyr^{673} and Tyr^{728} to phenylalanine, a nonphosphorylatable amino acid, and tested whether any of the mutations would affect KSR1 phosphorylation by LCK. We found that the Y728F substitution greatly diminished, whereas Y673F increased KSR1 phosphorylation (Fig. 2, *B* and *C*). Along with the MS data of the present study, these results suggest that Tyr^{728}, but not Tyr^{673}, is the major target for LCK-mediated phosphorylation of KSR1.

Tyr^{673} Is Important for the Functional Conformation of the KSR1 Kinase Domain—Tyr^{673} and Tyr^{728} are located within the kinase domain of KSR1 (Fig. 3, *A* and *B*), which has been shown

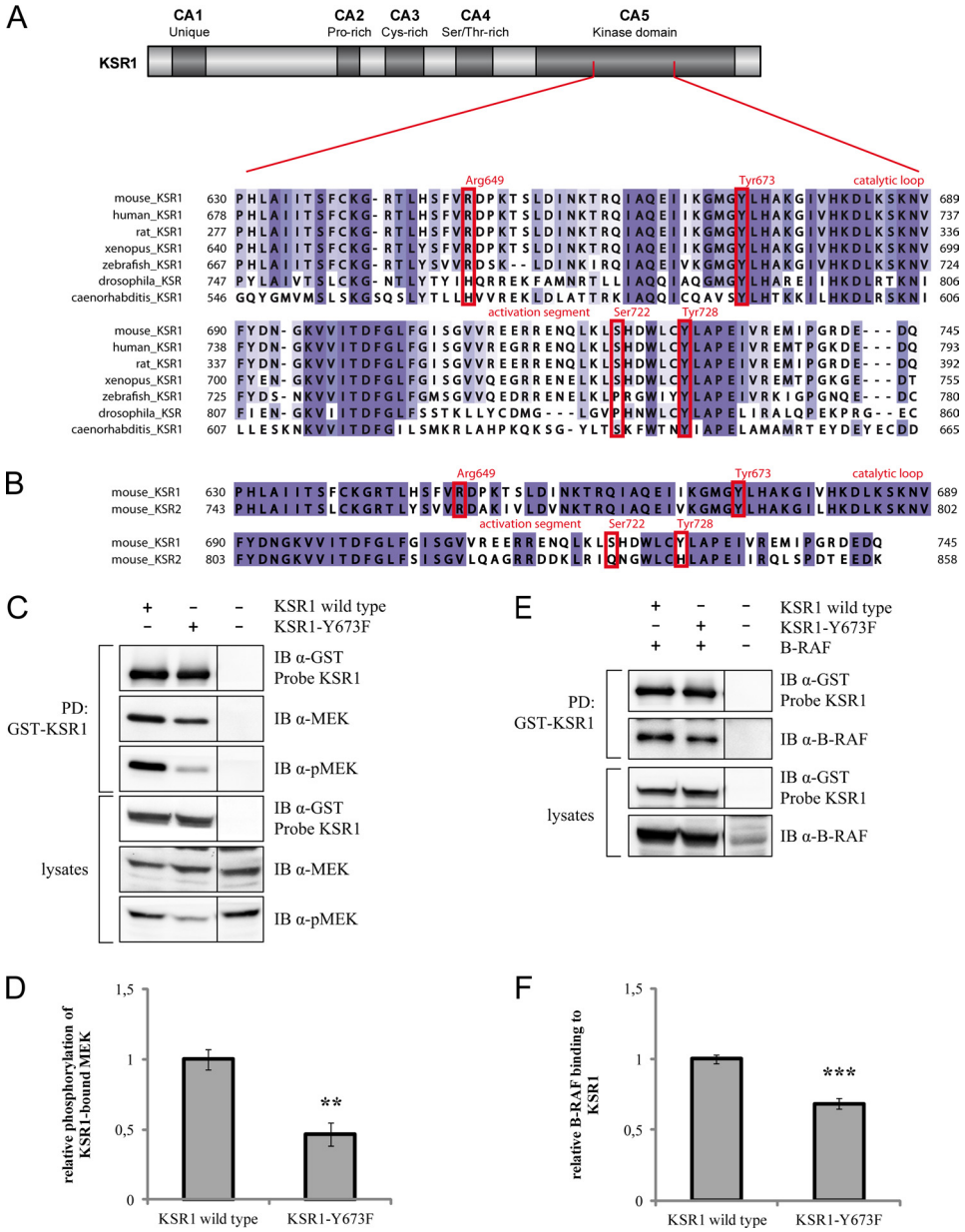

FIGURE 3. **Tyr[673] is crucial for maintaining the structure of the KSR1 kinase domain.** *A*, schematic presentation of KSR1 and multiple sequence alignment of KSR1 from different species. *B*, pairwise alignment of murine KSR1 and KSR2. The amino acid sequences were obtained from NCBI (accession numbers NP_038599, Q8IVT5, NP_001101754, NP_001186688, XP_684771, AAF52021, NP_509396, and NP_001108017) and merged with Jalview software. *C–F*, GST-tagged KSR1 WT or KSR1-Y673F mutant were transfected into COS7 cells. The cells were lysed and subjected to GST precipitation by use of glutathione-Sepharose beads. The amounts and phosphorylation levels of (co)precipitated proteins were determined by use of appropriate antibodies. For diagrams, data from three independent experiments were quantified by optical densitometry. Bar diagrams show the relative amount of phosphorylated MEK bound to KSR1, where 1-fold represents phosphorylation level of MEK interacting with KSR1 WT (*D*) or the relative amount of B-RAF bound to KSR1, where 1-fold represents B-RAF interacting with KSR1 WT (*F*). The data are presented as means ± S.D. of the respective measured parameters. *ns* (not significant), $p \geq 0.05$; * (significant), $p < 0.05$; ** (highly significant), $p < 0.01$; *** (extremely significant), $p < 0.001$ *versus* corresponding WT control. *PD*, pulldown; *IB*, immunoblot; α, anti.

to bind and prime MEK1 for activating phosphorylation by RAF kinases (13). Remarkably, whereas Tyr[673] is highly conserved between all KSR and RAF proteins, respectively, Tyr[728] is conserved only between KSR1 proteins of different species and is replaced by histidine in KSR2 (Fig. 3, *A* and *B*). Previously, the Tyr[673] homolog in *Drosophila* RAF (Tyr[538] in D-RAF) was also considered as a potential phosphorylation site but was not confirmed experimentally. It was suggested that as a highly conserved amino acid, Tyr[538] might be important for the functional structure of the D-RAF kinase domain. Indeed, it was shown that the Y538F mutation completely abolished the kinase activity of D-RAF (44). In light of these data, we assumed that Tyr[673] might be important for the structure of the KSR1 kinase domain, rather than being a regulatory phosphorylation site. To prove this assumption, we tested whether Tyr[673] modification is important for the binding of MEK and B-RAF to KSR1 and for activating phosphorylation of MEK by RAF. We found that Y673F substitution impaired both the binding of MEK and B-RAF to KSR1 (Fig. 3, *C*, *E*, and *F*). Moreover, phosphorylation of the KSR1-Y673F-bound MEK was strongly diminished compared with KSR1 WT-bound MEK, resulting in a reduced phospho-MEK level

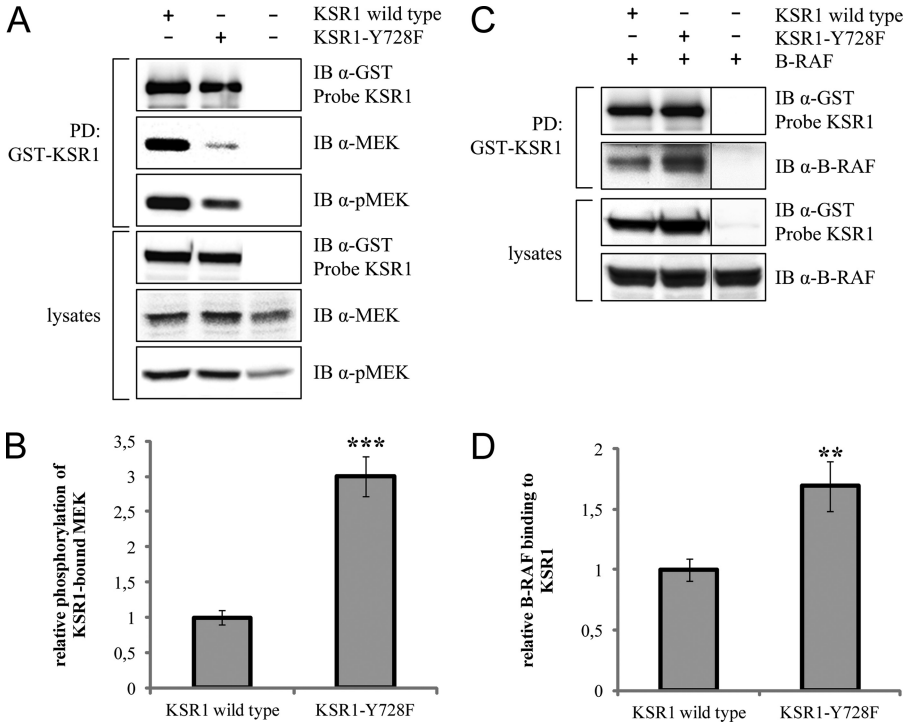

FIGURE 4. **Tyr[728] regulates activation of MEK.** *A* and *C*, GST-tagged KSR1 WT and KSR1-Y728F were transfected into COS7 cells and precipitated with glutathione-Sepharose beads. The amounts and phosphorylation levels of (co)precipitated proteins were determined by use of appropriate antibodies. For bar diagrams in *B* and *D*, data from three independent experiments were quantified as described in the legend to Fig. 3. *PD*, pulldown; *IB*, immunoblot; α, anti.

in lysates (Fig. 3, *C* and *D*). These results support the assumption that similar to Tyr[538] of D-RAF, Tyr[673] is important for maintaining the functional conformation of the KSR1 kinase domain.

Tyr[728] Regulates the Activating Phosphorylation of MEK—We next explored whether Tyr[728] is important for MEK activation. To this end, we tested the binding of MEK and B-RAF to KSR1-Y728F mutant and phosphorylation of KSR1-Y728F-bound MEK in a coprecipitation assay. The results of these experiments revealed that although the binding of MEK to KSR1 was dramatically reduced by Y728F substitution, the activating Ser[218] and Ser[222] phosphorylation of the KSR1-Y728F-bound MEK was three times higher than the phosphorylation of MEK bound to KSR1 WT (Fig. 4, *A* and *B*). Furthermore, binding of B-RAF to KSR1-Y728F mutant was increased compared with WT (Fig. 4, *C* and *D*). These results are consistent with the idea that Tyr[728] of KSR1 plays a regulatory role in the mechanism of MEK activation and suggest that phosphorylation of Tyr[728] may interfere with the activating phosphorylation of MEK by B-RAF.

Phosphorylation of Tyr[728] Negatively Regulates Cell Proliferation—KSR is known as a general positive mediator of MAPK signaling. ERK stimulation in the absence of KSR was attenuated in a variety of systems, including tumor growth and T cell activation (16). Our experimental data suggest that phosphorylation of KSR1 on Tyr[728] negatively regulates MEK activation by B-RAF and may result in inhibition of cellular processes depending on MAPK signal transduction. To test the effect of Tyr[728] phosphorylation on cell proliferation, we used MEFs derived from KSR1-deficient mice (KSR1$^{-/-}$ MEFs) (16, 45). KSR1$^{-/-}$ MEFs were infected with retroviruses for stable expression of KSR1 WT or KSR1-Y728F mutant. As shown in Fig. 5, proliferation of MEFs stably expressing KSR1 WT was almost unchanged compared with MEFs infected with empty vector. In contrast, MEFs expressing KSR1-Y728F proliferated significantly faster than MEFs infected with KSR1 WT. These results are consistent with the data showing that Y728F substitution increases activating phosphorylation of KSR1-bound MEK by B-RAF (Fig. 4), supporting the assumption that phosphorylation of Tyr[728] in KSR1 may interfere with the B-RAF-mediated activation of MAPK signaling and as a consequence delay cell proliferation.

Conformational Rearrangement of the KSR1 Kinase Domain Is Required for Phosphorylation of Tyr[728]—To obtain insights into possible mechanisms by which Tyr[728] phosphorylation may regulate the function of KSR1, we performed modeling of KSR1 kinase domain (KD) with and without Tyr[728] phosphorylation. In addition, a homology model for the interaction of KSR1(KD) with MEK1 was built. For modeling, we used the recent structure analysis of the protein-protein complex of human KSR2(KD) bound to rabbit MEK1 as a template (13). Because of the very high homology between the kinase domains of mouse KSR1 and human KSR2, comprising 69% sequence identity on the amino acid level (86% sequence homology), the KSR1(KD) model could be built without requiring manual loop building or modeling of deletions and thus provides a valid KSR1(KD) model for further structural and functional analyses. The modeling revealed that in the bound conformation, as in KSR2(KD) in complex with MEK1, the Tyr[728] of KSR1(KD), which is located in a short helical element just C-terminal of the activation segment and ahead of αEF helix, is buried inside the core of the kinase domain (Fig. 6, *A* and *B*). This suggests that for phosphorylation of Tyr[728], a conformational rearrangement

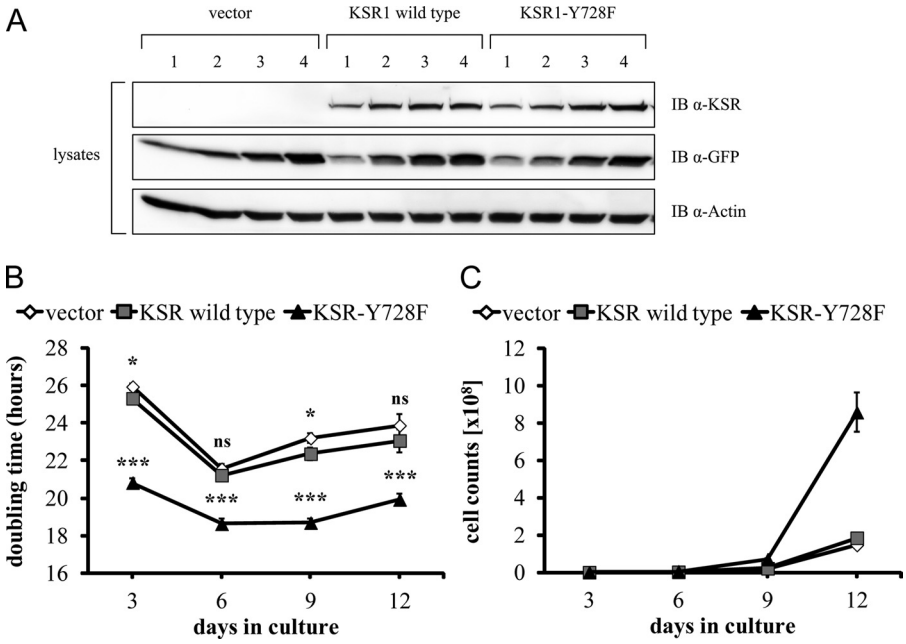

FIGURE 5. **Substitution of Tyr[728] in KSR1 promotes proliferation of MEFs.** KSR1$^{-/-}$ MEFs were infected with retroviruses carrying empty vector, KSR1 WT, or KSR1-Y728F. Infected MEFs were sorted by FACS according to the levels of GFP fluorescence. Four fractions of infected MEFs were collected, and KSR1 expression was tested by immunoblotting (*A*). For proliferation assay, fraction number 4 was used. Proliferation of infected MEFs was analyzed by counting living cells using FACS on days 3, 6, 9, and 12 after synchronization of cell cycle. During the time frame of the assay MEFs were kept in the exponential growth phase by trypsinizing and seeding every third day. The cell counts were used to calculate the population doubling time (*B*) and determine the cell proliferation curves (*C*) as described in Ref. 53. *Points*, mean of at least three independent experiments; *bars*, S.D. *ns* (not significant), $p \geq 0.05$; * (significant), $p < 0.05$; ** (highly significant), $p < 0.01$; *** (extremely significant), $p < 0.001$ *versus* corresponding empty vector control.

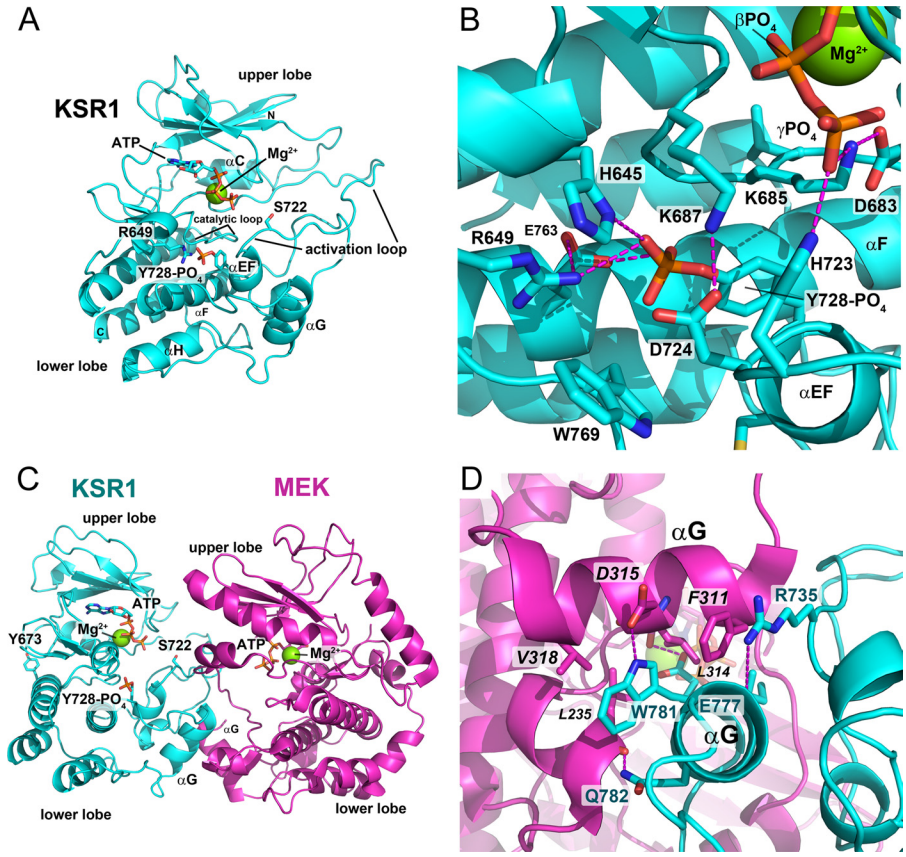

FIGURE 6. **Structure of the mKSR1-MEK1 kinase domain complex with focus on Tyr(P)[728].** *A*, overall view of the mKSR1(KD) modeled by use of the structure of hKSR2(KD) as a template (13). *B*, detailed view of direct hydrogen bonds formed between the phosphate group of Tyr(P)[728] and the surrounding residues in mKSR1(KD). *C*, overall view of the mKSR1-MEK1 complex modeled by docking the structure of mKSR1(KD) from *A* onto the template complex KSR2-MEK1 (13). *D*, close-up view of the interacting surface in mKSR1(KD) and MEK1(KD).

compared with the bound conformation of KSR2(KD) in complex with MEK1 (Protein Data Bank entry 2Y4I) must occur. However, because the activation segment consists of a rather long loop with a large number of polar and/or charged residues and no stabilizing secondary structure, it seems very likely that in its unbound state (*i.e.*, not interacting with MEK1), the activation segment is not conformationally restrained, and thus Tyr^{728} might be placed at the protein surface accessible for phosphorylation by LCK. This interpretation is consistent with the observation that even in the complex of KSR2(KD) bound to MEK1, a part of the activation segment of KSR2(KD) has no observable electron density because of disorders (13). In contrast, Tyr^{673} is also partially buried in the kinase domain, but in comparison to Tyr^{728}, it is a part of a conformationally restrained helical element (Fig. 6*C*). Therefore, it is most likely that Tyr^{673} is not accessible to modification by tyrosine kinases, which is in accordance with our results obtained for substitution.

The model of KSR1 in Fig. 6*B* also shows that the phosphomoiety of $Tyr(P)^{728}$ forms a network of direct hydrogen bonds with several surrounding residues located in helical elements, such as αD helix (His^{645} and Arg^{649}) and αF helix (Glu^{763}). Arg^{649} might serve as an anchor point for the phosphate group of $Tyr(P)^{728}$. When the KSR1(KD)-$Tyr(P)^{728}$ model was compared with a model containing a nonphosphorylated Tyr^{728} residue, no direct hydrogen bonds between the tyrosine hydroxyl group and surrounding residues could be found. This might hint toward a (locally) increased stability of the KSR1(KD) structure when Tyr^{728} is phosphorylated, which in turn might alter MEK and/or RAF binding. The model-derived prediction is consistent with the experimental data obtained for Y728F mutant, which showed strongly reduced MEK binding but increased interaction with B-RAF (Fig. 4, *A*, *C*, and *D*).

Additionally, to test whether the interaction between KSR1(KD) and MEK differs significantly from the KSR2(KD)/MEK interaction shown in the published structure analysis (13), we have docked the model obtained for murine KSR1(KD) onto the template complex KSR2(KD)-MEK1 (Protein Data Bank entry 2Y4I). The kinase-kinase interface is located in the lower lobes of both kinases and the contact between the αG helices of both kinase domains contributes the largest surface to this interaction (Fig. 6, *C* and *D*). Interestingly, all residues in this helix, which are in direct contact with residues of MEK1, are invariant between KSR1 and KSR2, indicating that the interaction mechanism for this kinase-kinase interaction is likely to be highly similar.

Arg^{649} Stabilizes the Bound Conformation of KSR1 Kinase Domain in Complex with MEK—Next, we tested, whether substitution of Arg^{649} (a predicted anchor point for the phosphate group of $Tyr(P)^{728}$) with alanine or glutamic acid might impair stability of the KSR1 kinase domain and thereby alter the KSR1/MEK interaction. The results of this experiment revealed that similar to KSR1-Y728F mutant, substitution of Arg^{649} either strongly reduced (R649A) or completely abolished (R649E) the KSR1/MEK association (Fig. 7*A*). These data support the model-derived assumption that Arg^{649} might be involved in stabilization of the bound conformation of KSR1 kinase domain in complex with MEK. Consistent with this idea, we found that exchange of Arg^{649} resulted in increased binding of LCK to KSR1 leading to a remarkably higher Tyr^{728} phosphorylation level compared with KSR1 WT (Fig. 7*A*). This suggests that amino acid exchanges at position 649 might shift the equilibrium of KSR1 folding states toward the conformation, in which Tyr^{728} is placed at the protein surface, accessible for phosphorylation by LCK.

Chemical Structure of the Amino Acid at Position 728 Determines Functional Properties of KSR1—We have shown that the MEK binding ability of KSR1 mutants Y728F and R649A is strongly reduced compared with WT (Figs. 4*A* and 7*A*). However, these substitution mutants behaved differently with respect to phosphorylation of KSR1-bound MEK. Whereas the phosphorylation of the KSR1-R649A-bound MEK was unchanged, the phosphorylation of MEK in the complex with KSR1-Y728F was three times higher than the phosphorylation of MEK bound to KSR1 WT (compare Fig. 7*A* with Fig. 4*A* and *B*). To test whether this effect is specific for tyrosine to phenylalanine exchange or is general for substitution with any amino acid at this position, we generated Y728A and Y728E substitutions in KSR1 and analyzed their competence for MEK binding and phosphorylation of KSR1-bound MEK. We found that similar to the substitution with phenylalanine, the MEK binding to Y728A mutant was significantly reduced, whereas the phosphorylation of KSR1-Y728A-bound MEK was markedly increased compared with WT. Substitution of Tyr^{728} with negatively charged glutamic acid completely abolished binding of MEK to KSR1 (Fig. 7, *B* and *C*). Interestingly, in KSR2 the Tyr^{728} of KSR1 is replaced by histidine (His^{841}; see also Fig. 3*B*). Therefore, we decided to test whether substitution of Tyr^{728} to histidine may have any effect on KSR1 functionality. Surprisingly, Y728H mutation did not change the association between KSR1 and MEK, but it significantly reduced the phosphorylation of KSR1-bound MEK (Fig. 7, *B* and *C*). Taken together, our substitution analysis revealed that the amino acid at position 728 has a dual importance for the functional properties of KSR1. First, it is involved in maintaining the bound conformation of KSR1 kinase domain in complex with MEK and therefore influences KSR1/MEK association. Second, it affects phosphorylation of MEK. Our results also suggest that these two functions are in reciprocal relation to each other. The chemical structure of the amino acid at position 728, which favors the tight binding of MEK, reduces phosphorylation of the bound MEK and vice versa.

Phosphorylation of Tyr^{728} Induces Conformational Rearrangements in the MEK Interface and Affects Structural Elements Involved in Catalytic Activity of KSR1—To test whether and how phosphorylation of Tyr^{728} in KSR1 might alter structure, potential kinase activity, or the interaction of KSR1 with MEK, we performed MD simulations in explicit water. The model of the KSR1(KD) with or without Tyr^{728} phosphorylated was placed in a water box with ions at a concentration of 150 mM to neutralize protein charges, and 5-ns unrestrained trajectories were calculated after stepwise minimization. Using visual molecular dynamics hydrogen bonding and r.m.s. deviation, fluctuations were checked for various elements in the kinase domain (Fig. 8). As suggested from the static starting model, hydrogen bonding between the side chain of Tyr^{728} and sur-

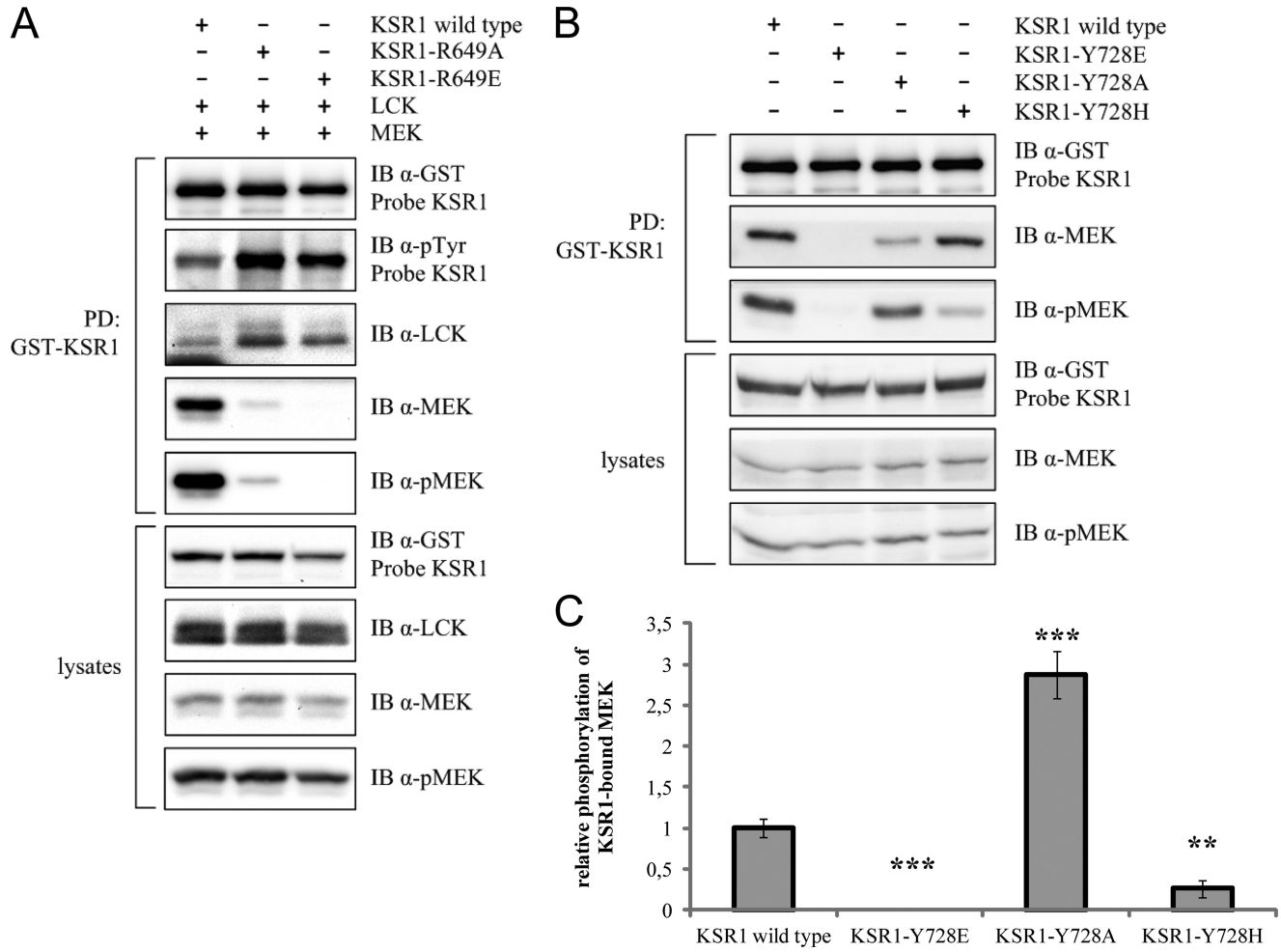

FIGURE 7. **Substitution of Arg[649] and Tyr[728] with different amino acids results in distinct outcomes for MEK binding and phosphorylation.** *A* and *B*, GST-KSR1 WT and the indicated mutants were expressed in COS7 cells and precipitated by use of glutathione-Sepharose beads. The amounts and phosphorylation levels of (co)precipitated proteins were determined by use of appropriate antibodies. *C*, data from three independent experiments were quantified by optical densitometry. The bar diagram shows the relative amount of phosphorylated MEK bound to KSR1, where 1-fold represents phosphorylation level of MEK interacting with KSR1 WT. The data are presented as means ± S.D. of the respective measured parameters. *ns* (not significant), $p \geq 0.05$; * (significant), $p < 0.05$; ** (highly significant), $p < 0.01$; *** (extremely significant), $p < 0.001$ *versus* corresponding WT control. *PD*, pulldown; *IB*, immunoblot; α, anti.

rounding residues was stronger in case of the Tyr(P)[728] throughout the 5-ns trajectory, in both the numbers of hydrogen bonds as well as the duration of hydrogen bonding. This suggests that the helical element containing Tyr(P)[728] as well as elements, which are in contact with Tyr(P)[728], are possibly stabilized. The r.m.s. deviation analysis of the helix, which carries Tyr[728] at its C-terminal end, shows that in the case of Tyr(P)[728] the conformational and positional variations of the backbone atoms are significantly lower (r.m.s. deviation, ~2 Å) compared with KSR1 with the nonphosphorylated Tyr[728] (r.m.s. deviation, between 2 and 4 Å; see Fig. 8*B*). Other regions, similarly, appear less flexible in the MD simulations of KSR1 with Tyr(P)[728]. For example, the activation loop (residues Ser[707]–His[723]), which in kinases usually controls the access of the substrate to the active site and is displaced by phosphorylation of serine and/or threonine residues present in this segment, exhibits lower fluctuations for the backbone atoms when Tyr[728] is phosphorylated (Fig. 8*C*). This may indicate that phosphorylation of Tyr[728] leads to stabilization of the activation segment, which in turn potentially influences KSR1 kinase activity and/or stabilizes complex formation with MEK. Consistent with a potential effect on kinase activity is the observation that in KSR1 with phosphorylated Tyr[728], the Lys[685], which is involved in phosphate transfer, interacts with the phosphate group of Tyr(P)[728] and thus exhibits a highly restrained side chain conformation throughout the 5-ns trajectory, whereas for KSR1 with nonphosphorylated Tyr[728], the lysine residue is far more flexible (Fig. 9, *A* and *B*). Other elements appear to be not affected significantly according to the MD simulation results. For example, the short helical element comprising Thr[643] to Arg[649], of which the latter residue might serve as an anchor point for the phosphate group of Tyr(P)[728], does not show any differences with respect to r.m.s. deviations of its backbone atoms (Fig. 8*D*). Neither does the catalytic loop segment carrying the conserved Asp[683] and Lys[685] residues, which are involved in transfer of the γ-phosphate group of the ATP onto the substrate, show a more stable backbone conformation when Tyr[728] is phosphorylated (Fig. 8*E*).

To gain insights on whether the Tyr[728] phosphorylation exerts a long range effect by modulating the stability of the interface either to MEK (αG helix consisting of residues Glu[777] to Ser[785]) or the potential binding site to the regulatory RAF

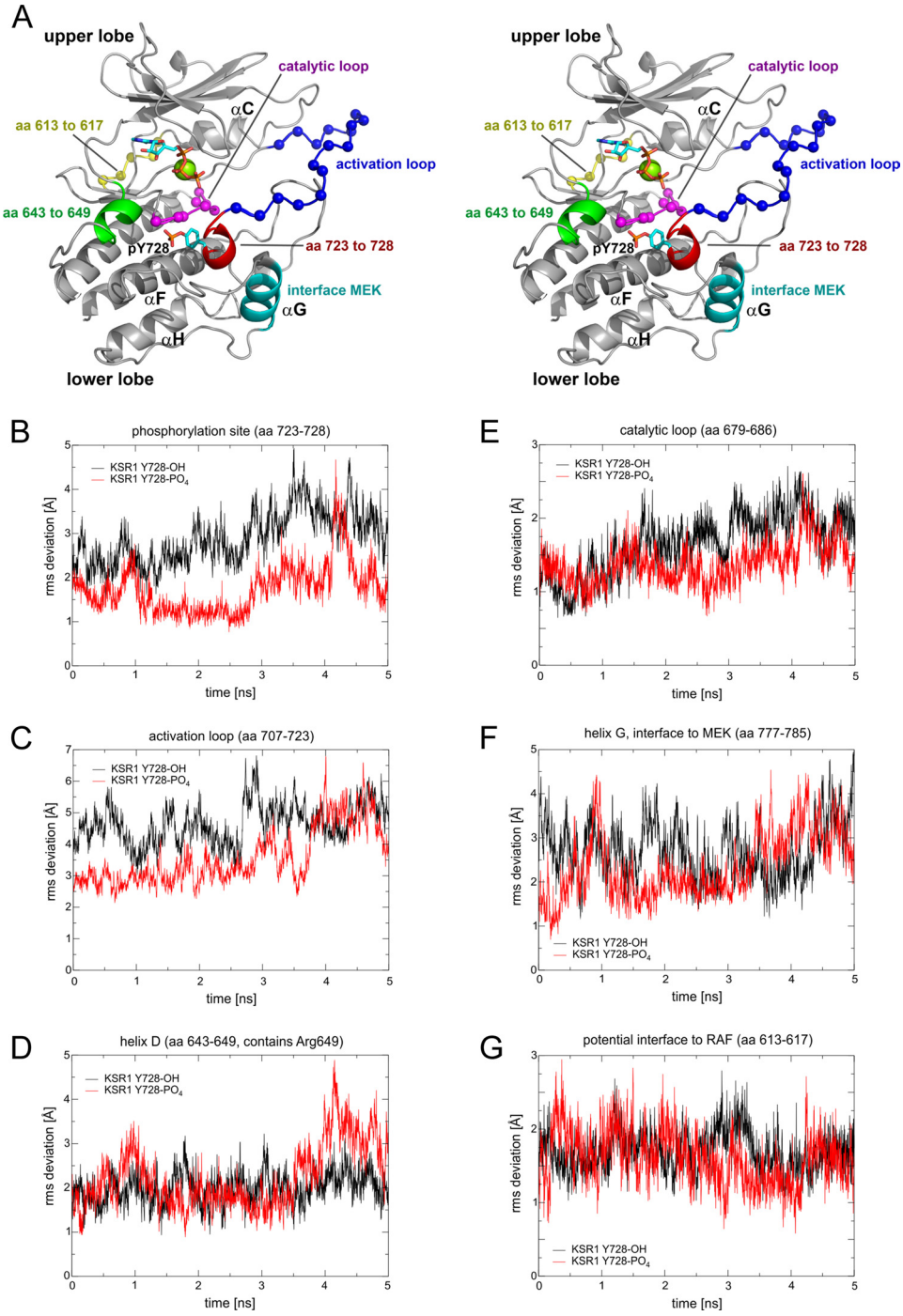

FIGURE 8. **Fluctuations of backbone coordinate in Tyr[728]-phosphorylated and Tyr[728]-nonphosphorylated KSR1 analyzed by MD simulations.** *A*, the model of the mKSR1(KD) (stereo view). The structural elements analyzed by MD simulation are highlighted in different colors. *Red*, helical element harboring Tyr[728]; *dark blue*, activation loop; green, the short helix comprising residues 643–649; *magenta*, catalytic loop (residues 679–686); *cyan*, αG helix (which is part of the KSR1 interface to MEK1); *yellow*, potential interface to RAF kinases. The Tyr(P)[728] and ATP moieties are shown as *sticks*; the magnesium ion is indicated as a *green sphere*. The loop regions are highlighted with the Cα atoms shown as *small spheres*. *B–G*, r.m.s. deviation for backbone atoms of indicated structural elements during the 5-ns trajectory molecular dynamics simulation using the software NAMD (Scalable Molecular Dynamics software package). The *curves* representing backbone atom fluctuations of Tyr[728]-nonphosphorylated KSR1(KD) are shown in *black*; the *red curves* represent the same of Tyr[728]-phosphorylated KSR1(KD). *aa*, amino acids.

kinase (loop element ahead of αC helix, residues Gln[613]–Glu[617]), we analyzed the fluctuations of the backbone atoms in the trajectories of both models, KSR1-Tyr[728] and KSR1-Tyr(P)[728]; however, no significant differences could be observed in the r.m.s. deviation (Fig. 8, *F* and *G*). Although the phosphorylation of Tyr[728] does not lead to stabilization of the KSR1/MEK1 interface, analysis of the distances between the Cα atom of Tyr[728] and Ala[778], which is on the MEK facing side of the αG helix and one of the KSR1 residues contacting MEK1, shows that in KSR1 with Tyr(P)[728], the Cα-Cα distance is shorter throughout the MD simulation compared with KSR1 with nonphosphorylated Tyr[728] (Fig. 9, *C* and *D*). Thus, a con-

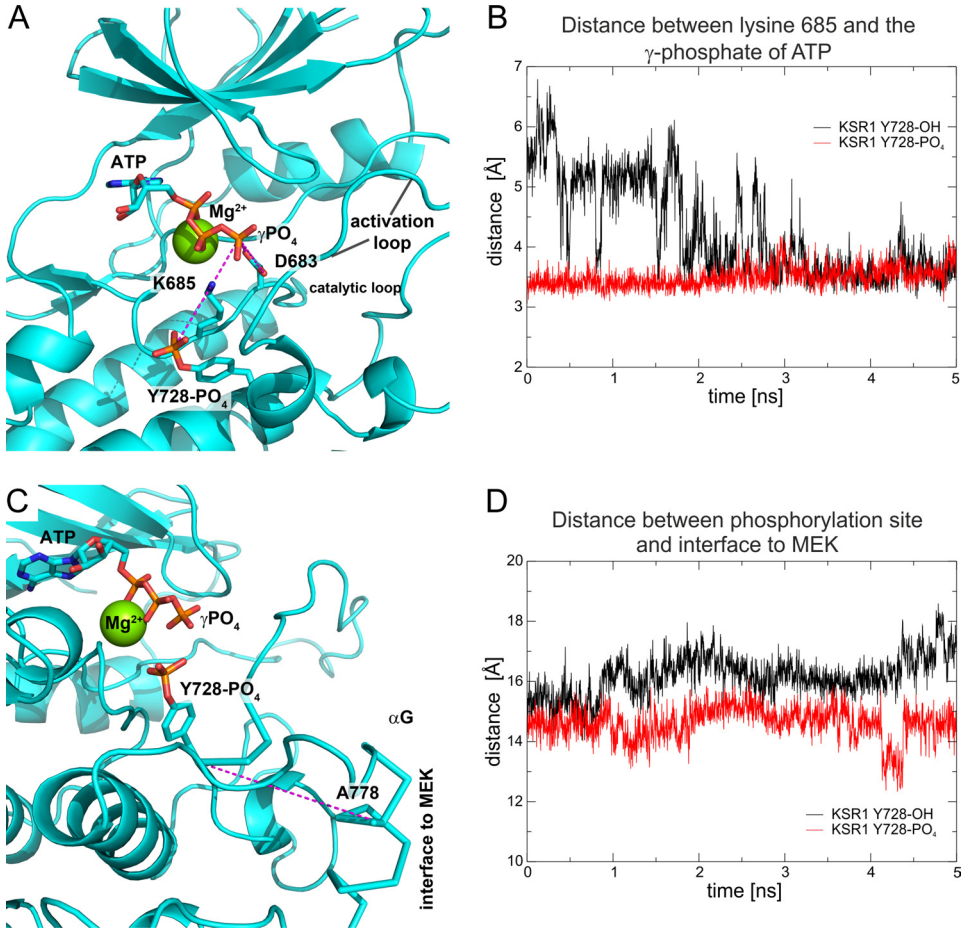

FIGURE 9. **MD simulations suggest that phosphorylation of Tyr[728] may alter KSR1 kinase activity or/and its interaction with MEK.** *A*, close-up view of the polar interactions between the phosphate group of Tyr(P)[728] and the conserved Lys[685] in the catalytic loop of KSR1(KD). The ATP and magnesium ion are presented as *ball and stick models* (also in *C*); the Asp[683], which is also involved in the phosphate transfer, is shown as *sticks*. *B*, the variation in distance between the amino nitrogen atom of Lys[685] and the γ-phosphate atom of the ATP molecule is shown for Tyr[728]-phosphorylated (*red curve*) and Tyr[728]-nonphosphorylated KSR1(KD) (*black curve*). During the trajectory of the MD simulation, the amino group of the conserved Lys[685] in the catalytic loop of KSR1(KD) becomes conformationally fixed between the phosphate group of Tyr(P)[728] and the γ-phosphate group of the ATP molecule, such that it can ideally facilitate phosphate transfer from the ATP to an acceptor hydroxyl group in a substrate (*red curve*). In case of Tyr[728] being not phosphorylated, the distance between the amino group of Lys[685] and the γ-phosphate of the ATP molecule varies throughout the MD simulation, indicating that the groups involved in the catalytic cycle of phosphate transfer are not properly lined up over time (*black curve*). *C*, close-up view of the potential long range interaction between Tyr(P)[728] and the αG helix of KSR1, which is the major contact surface in the KSR1(KD)/MEK1 interaction. *D*, to analyze possible conformation rearrangements in the αG helix, the variation in distance between the Cα atom of Tyr[728] and Ala[778] was monitored throughout the 5-ns trajectory of the molecular dynamics simulation. The comparison of the distance variation between Tyr[728]-phosphorylated (*red curve*) and Tyr[728]-nonphosphorylated KSR1(KD) (*black curve*) indicated that with Tyr[728] being phosphorylated the distance between Tyr[728] and the αG helix of the KSR1(KD) is smaller and a more compact interface might facilitate MEK1 binding.

formational rearrangement most likely induced by the higher stability of the activation loop in KSR1-Tyr(P)[728] leads to a more compact KSR1/MEK1 interface.

DISCUSSION

In the present study, we have investigated the mechanism of KSR1 regulation by both structural modeling and biochemical means. We have identified a novel tyrosine residue (Tyr[728]) within the KSR1 kinase domain, which is phosphorylated by the Src kinase family member LCK and is important for binding and phosphorylation of MEK *in vivo*. Structure modeling revealed that in the bound conformation of KSR1 in complex with MEK, the Tyr[728] is packed inside the core of the kinase domain and is likely not accessible to phosphorylation. This means that conformational rearrangement of the KSR1 kinase domain is required for placing the Tyr[728] at the protein surface and making it accessible to modification by a tyrosine kinase. This consideration was confirmed by our experimental data. Arg[649], which is conserved in KSR1 and KSR2, is thought to stabilize the bound conformation of KSR1 kinase domain, because the cationic side chain of Arg[649] is an anchor point for the phosphate residue of Tyr(P)[728], and it also possibly interacts with Trp[769] (Fig. 6*B*). The latter so called cation-π interaction between the cationic side chain of an aliphatic amino acid and the side chain of an aromatic residue can significantly contribute to the stabilization of the protein secondary structure (46). Therefore, replacement of Arg[649] was expected to relax the protein structure around the Tyr[728] and make it accessible for phosphorylation. Indeed, substitution of Arg[649] to alanine or glutamic acid led to enhanced binding of LCK accompanied by increased phosphorylation of Tyr[728] (Fig. 7*A*). Similar to the data obtained for Arg[649], replacement of Tyr[673] with phenylalanine resulted in increased phosphorylation of Tyr[728] (Fig. 2*B*). Tyr[673] is highly conserved not only in KSR but also in RAF

proteins and is considered to be important for maintaining the functional conformation of the kinase domain (44). Therefore, it is most likely that substitution of Tyr^{673} leads to partial unfolding of the kinase domain placing Tyr^{728} at the protein surface accessible for phosphorylation by LCK.

Phosphorylation of buried residues is not unique to KSR1. A substantial number of phosphorylation sites (15%) are actually packed into the domain core of proteins and not exposed to the solvent (47). The systematic comparative and structural analysis of phosphorylatable buried residues revealed that their modifications could have three major structural/functional effects: (i) regulation of function by affecting functional sites directly or indirectly, (ii) spatial rearrangements (presumably by rigid body movements) of domains within a protein, and (iii) opening of the structure, leading to local flexibility (47). Frequently, phosphorylatable buried residues are found at or close to active sites and binding pockets of proteins. There are numerous examples demonstrating that their phosphorylation affects either directly or indirectly the integrity of the functional sites depending on whether they are part or in the vicinity of them, respectively (47). According to the model of KSR1(KD) shown in Fig. 6, Tyr^{728} is located close to the catalytic loop and activation segment. These functional elements are present in every known protein kinase. The invariant aspartic acid of the catalytic loop (Asp^{683} in KSR1; see Fig. 3, *A* and *B*) is presumed to act as a catalytic base to free up the hydroxyl oxygen on the substrate for nucleophilic attack (Figs. 6*B* and 9*A*). The activation loop often contains a phosphorylation site that upon phosphorylation induces a conformational change on the loop that allows the substrate to bind to the kinase and also positions the invariant aspartate group of the catalytic loop for phosphate transfer reaction (48). The close proximity of Tyr^{728} to these functional elements suggests that phosphorylation of this residue may influence the potential catalytic competence of KSR1. Indeed, our MD simulations support this assumption. The backbone atoms of the activation loop exhibit lower fluctuations when Tyr^{728} is phosphorylated (Fig. 8*C*). Moreover, the amino group of the conserved Lys^{685} in the catalytic loop seems conformationally fixed between the phosphate group of $Tyr(P)^{728}$ and the γ-phosphate group of the ATP molecule, such that it can ideally facilitate phosphate transfer from the ATP to an acceptor hydroxyl group in a substrate (Fig. 9, *A* and *B*). Substitution of arginine for the conserved ATP-coordinating lysine residue in mammalian KSR proteins and the capacity of kinase-impaired mutants of KSR to mediate MEK phosphorylation and MAPK signaling have implicated KSR as a pseudokinase (10, 15). However, the protein structure of KSR2(KD) in complex with MEK1 indicates that KSR has the potential for catalytic activity (13). Indeed, it has been reported that KSR2 is the major kinase responsible for MEK1 phosphorylation at non-B-RAF sites (13). KSR2 is also capable to phosphorylate MEK1 at B-RAF sites (Ser^{218} and Ser^{222}), however, with extremely low efficiency (13). Other groups reported kinase activity for KSR1 (11, 12, 49). Thus, a growing body of evidence supports the view that KSR can indeed act as a protein kinase. Therefore, implication of Tyr^{728} phosphorylation in regulation of KSR1 catalytic activity seems very likely.

The published structure of the KSR2(KD)/MEK1 heterodimer revealed that these two molecules interact with their catalytic sites facing each other through their activation segments and αG helices (13). Therefore, changes in the conformation of the activation segment in the kinase domain of KSR are supposed to affect not only the catalytic competence of KSR but also its ability to bind MEK. As mentioned before, our static model of the KSR1(KD) bound to MEK revealed that Tyr^{728} is located in a short helical element just C-terminal of the activation segment. The hydroxyl group of the nonphosphorylated Tyr^{728} forms a network of interactions with surrounding residues, which may stabilize the conformation of the activation segment required for the binding to MEK. Indeed, substitution of Tyr^{728} with phenylalanine or alanine, the neutral residues that do not form any stabilizing interactions with surrounding residues in our model, resulted in strongly reduced MEK binding to KSR1 (Figs. 4*A* and 7*B*). Phosphorylated Tyr^{728} may stabilize the functional conformation of the activation segment even more efficiently, because the network of interactions is extended by several direct hydrogen bonds between the phosphate group and the surrounding residues. According to our model, a phosphomimetic amino acid, such as glutamic acid, at position 728 would not substitute for phosphorylated Tyr and also not for nonphosphorylated Tyr in terms of stabilization of the activation segment, because its predicted pattern of interactions with surrounding residues differs substantially from that of Tyr and Tyr(P). Consistently, the replacement of Tyr^{728} with glutamic acid completely abolished binding of KSR1 to MEK (Fig. 7*B*). Moreover, our MD simulations revealed that the distance between the Cα atom of Tyr^{728} and Ala^{778} residue of the αG helix is smaller, if Tyr^{728} is phosphorylated (Fig. 9, *C* and *D*). Thus, a more compact interface might be formed, possibly facilitating MEK binding to KSR1. Together, our data strongly suggest that chemical properties of the amino acid at position 728 may define the flexibility of the activation segment over time and as a consequence affect the stability of the interaction between the KSR1 kinase domain and MEK.

KSR/MEK heterodimers assemble KSR/MEK heterotetramers or KSR-MEK-RAF ternary complexes via side to side dimerization of two KSR molecules or of KSR and RAF molecules, respectively. It has been suggested that in the KSR/MEK heterotetramer, the inaccessible activation segment of MEK is released through the interaction of KSR with a regulatory RAF molecule, allowing catalytic RAF to phosphorylate MEK (13). Our experimental data are in agreement with this hypothesis. We have shown that substitution of the tyrosine at the position 728 with phenylalanine, which is supposed to loosen the KSR1/MEK interaction, facilitated the KSR1/B-RAF heterodimerization and increased the activating phosphorylation of the KSR1-bound MEK (Fig. 4).

The MS analysis of the present study further identified Ser^{722} as a novel phosphorylation site of KSR1 (Fig. 2*A*). Phosphorylation of this residue was found in all replicates, suggesting that Ser^{722} is one of the major phosphorylation sites in mouse KSR1. Remarkably, Ser^{722} is located six residues ahead of Tyr^{728} in the linear sequence of amino acids and is part of the activation loop (Figs. 3*A* and 6*A*). Therefore, we propose that the phosphorylation of Ser^{722} may affect catalytic activity and/or substrate

specificity of KSR1. Even more remarkable is the close proximity of Ser[722] to the catalytic site in the model of KSR1(KD) (Fig. 6*A* and *C*). Considering this fact, it is tempting to hypothesize that Ser[722] might be an autophosphorylation site. Previous studies revealed that mammalian KSR1 is indeed capable of serine autophosphorylation, which likely occurs on a single or limited number of serine residues, because only a single migrating ^{32}P-labeled peptide was detected in two-dimensional tryptic phosphopeptide mapping following *in vitro* kinase assay (49). Interestingly, Ser[722] is conserved in KSR1 proteins of different species but is replaced by a nonphosphorylatable amino acid (Gln[835]) in KSR2 (Fig. 3, *A* and *B*). Consistently, no autophosphorylation of KSR2 has been reported so far. Taken together, the assemblage of facts supports the idea that Ser[722] might be autophosphorylated in *cis*. In general, autophosphorylation of a critical residue in the activation loop is an essential maturation event required for full enzyme activity of several protein kinases (50–52). Therefore, the autophosphorylation of Ser[722] may be crucial for the catalytic activity of KSR1. This assumption is supported by the observation that the substitution of the serine at the position 722 to alanine or aspartic acid did not change the interaction between KSR1 and MEK but strongly diminished the phosphorylation of KSR1-bound MEK (data not shown).

As pointed out before, there is no phosphorylation site in mammalian KSR2 at the position homologous to Ser[722] of KSR1. Intriguingly, the KSR1-Tyr[728] is also replaced by a nonphosphorylatable amino acid (His[841]) in KSR2 (Fig. 3*B*). The co-occurrence of these two substitutions in the course of KSR evolution supports the idea of a regulatory interrelation between the phosphorylation of Tyr[728] and Ser[722]. In general, kinases that are autophosphorylated in *cis* are likely to have developed additional mechanisms to regulate their activity, including phosphorylation on other regions of the kinase (52). Phosphorylation of Tyr[728] might be such an additional regulatory mechanism of the KSR1 kinase activity. Loss of the autophosphorylation site Ser[722] in the activation segment would make the Tyr[728]-mediated regulation redundant. Therefore, mammalian KSR2, in which the autophosphorylation site in the activation segment was omitted, also lost the regulatory phosphorylation site at position homologous to Tyr[728] of KSR1.

A previous study of the molecular mechanism, by which protein kinases phosphorylate their own activation loop, suggests that a canonical kinase domain can adopt a functional intermediate during maturation of the enzyme (52). As discussed before, the existence of such an intramolecular transitional intermediate is a *conditio sine qua non* for phosphorylation of KSR1-Tyr[728] by LCK. Therefore, we hypothesize that LCK phosphorylates the nascent KSR1 kinase passing through a transitory intermediate. Our static model and molecular dynamics simulations suggest that in the mature kinase, Tyr(P)[728] locally stabilizes the functional element involved in catalytic reaction (Figs. 6, 8, and 9) and consequently may increase the likelihood of the activating Ser[722] autophosphorylation resulting in enhanced catalytic activity of KSR1 toward MEK. In support of this hypothesis, we found that the replacement of tyrosine at the position 728 with histidine, whose uncharged form is isosterically analog to tyrosine, did not change the interaction between KSR1 and MEK but strongly decreased phosphorylation of the KSR1-bound MEK (Fig. 7, *B* and *C*). This suggests that histidine at the position 728 can be tolerated with respect to KSR1/MEK interaction, but not with respect to catalytic activity of KSR1. These data are in line with the observation that KSR2, which binds MEK as efficient as KSR1 but has very low intrinsic kinase activity toward MEK (13), has a histidine at the position homologous to KSR1-Tyr[728] (Fig. 3*B*).

In light of our results, we propose a model in which phosphorylation of Tyr[728] may regulate the transition between the scaffolding and the catalytic function of KSR1. Whereas autophosphorylation of Ser[722] would activate the kinase activity of KSR1 toward MEK, phosphorylation of Tyr[728] by LCK would facilitate the autophosphorylation of Ser[722], support the face to face binding of MEK to KSR1 for phosphorylation of MEK by KSR1, and counteract the side to side heterodimerization of KSR1 with a regulatory RAF molecule preventing the release of MEK activation segment for phosphorylation by catalytic RAF.

In this work, we show that the proliferation of KSR1-deficient MEFs infected with the KSR1-Y728F mutant was significantly increased in comparison to MEFs infected with KSR1 WT (Fig. 5), although the overall MEK and ERK phosphorylation in the lysates was unchanged (data not shown). Because LCK is expressed specifically in lymphocytes, which other tyrosine kinase(s) come(s) into question for phosphorylation of the KSR1-Tyr[728] in MEFs? One possible candidate might be c-Src. Indeed, it has been previously shown that, for example, Tyr[340/341] in C-RAF and the analog residues in A-RAF can be phosphorylated by both c-Src and LCK (32, 33, 54), suggesting that these two kinases share similar substrates. Furthermore, Kilkenny *et al.* (55) reported that MEFs expressing endogenous c-Src exhibit significantly higher FGF- and EGF-induced proliferation rates than cells lacking c-Src, whereas overexpression of c-Src reduced cell proliferation to the level of c-Src knockout MEFs. This indicates that c-Src has positive as well as negative regulatory effects on FGF and EGF signaling. Interestingly, despite the difference in cell proliferation, the level of ERK activation was similar in cells with either endogenous expression or overexpression of c-Src (55). Although the mechanism underlying the negative effects of c-Src overexpression were not addressed in the study by Kilkenny *et al.* (55), our data suggest that phosphorylation of KSR1-Tyr[728] by c-Src might be one possible mechanism. This assumption is supported by the previously published observation that KSR1 specifically blocks growth factor and RAS-induced phosphorylation and activation of Elk-1 (a physiological substrate of ERK involved in regulation of cell proliferation, differentiation, and apoptosis), without affecting the overall activation of ERK itself (56). Of note, this effect of KSR1 on Elk-1 appears to require the integrity of its kinase domain, because a kinase-deficient mutant of KSR1 does not inhibit Elk-1 but even enhances both Elk-1 phosphorylation and transactivation activity in unstimulated cells (56). Moreover, KSR1 (the isoform whose function can be regulated by the lymphocyte-specific tyrosine kinase LCK), but not KSR2, is essential for proper activation of the MAPK pathway and biological output in primary T lymphocytes (57). It has been reported that KSR1 modulates the sensitivity of MAPK

pathway activation in T cells without altering fundamental system outputs. Accordingly, the level of KSR1 expression is carefully regulated during T cells maturation relative to the components of the MAPK module (57). The results from our proliferation experiments, taken together with the above-described conclusions from other authors, suggest that Tyr^{728} phosphorylation of KSR1 by LCK is of major physiological relevance and not a simple artifact of transient transfection and/or overexpression. In conclusion, we have identified a novel regulatory phosphorylation site in KSR1, Tyr^{728}, and shown that this tyrosine is phosphorylated by LCK. Furthermore, we propose KSR1 as a control point used to fine-tune cellular responses by regulating the transition between its scaffolding and catalytic functions.

Acknowledgments—We thank Robert E. Lewis (University of Nebraska Medical Center, Omaha, NE) for generously providing the immortalized KSR1$^{-/-}$ *MEFs and the bicistronic FLAG-tagged murine KSR1 wild type construct as well as empty MSCV-IRES-GFP and ecotropic packaging vector; Ann-Cathrin Winkler and Christine Siegl (Department of Microbiology, University of Wuerzburg) for help with FACS analysis; and Walter Kolch (Systems Biology Ireland) and Mirko Hekman for critical reading of the manuscript.*

REFERENCES

1. Clapéron, A., and Therrien, M. (2007) KSR and CNK. Two scaffolds regulating RAS-mediated RAF activation. *Oncogene* **26,** 3143–3158
2. Udell, C. M., Rajakulendran, T., Sicheri, F., and Therrien, M. (2011) Mechanistic principles of RAF kinase signaling. *Cell Mol. Life Sci.* **68,** 553–565
3. Lozano, J., Xing, R., Cai, Z., Jensen, H. L., Trempus, C., Mark, W., Cannon, R., and Kolesnick, R. (2003) Deficiency of kinase suppressor of Ras1 prevents oncogenic ras signaling in mice. *Cancer Res.* **63,** 4232–4238
4. Therrien, M., Chang, H. C., Solomon, N. M., Karim, F. D., Wassarman, D. A., and Rubin, G. M. (1995) KSR, a novel protein kinase required for RAS signal transduction. *Cell* **83,** 879–888
5. Channavajhala, P. L., Wu, L., Cuozzo, J. W., Hall, J. P., Liu, W., Lin, L.-L., and Zhang, Y. (2003) Identification of a novel human kinase supporter of Ras (hKSR-2) that functions as a negative regulator of Cot (Tpl2) signaling. *J. Biol. Chem.* **278,** 47089–47097
6. Sundaram, M., and Han, M. (1995) The *C. elegans ksr-1* gene encodes a novel Raf-related kinase involved in Ras-mediated signal transduction. *Cell* **83,** 889–901
7. Kornfeld, K., Hom, D. B., and Horvitz, H. R. (1995) The *ksr-1* gene encodes a novel protein kinase involved in Ras-mediated signaling in *C. elegans*. *Cell* **83,** 903–913
8. Michaud, N. R., Therrien, M., Cacace, A., Edsall, L. C., Spiegel, S., Rubin, G. M., and Morrison, D. K. (1997) KSR stimulates Raf-1 activity in a kinase-independent manner. *Proc. Natl. Acad. Sci. U.S.A.* **94,** 12792–12796
9. Denouel-Galy, A., Douville, E. M., Warne, P. H., Papin, C., Laugier, D., Calothy, G., Downward, J., and Eychène, A. (1998) Murine Ksr interacts with MEK and inhibits Ras-induced transformation. *Curr. Biol.* **8,** 46–55
10. Stewart, S., Sundaram, M., Zhang, Y., Lee, J., Han, M., and Guan, K. L. (1999) Kinase suppressor of Ras forms a multiprotein signaling complex and modulates MEK localization. *Mol. Cell. Biol.* **19,** 5523–5534
11. Zhang, Y., Yao, B., Delikat, S., Bayoumy, S., Lin, X. H., Basu, S., McGinley, M., Chan-Hui, P. Y., Lichenstein, H., and Kolesnick, R. (1997) Kinase suppressor of Ras is ceramide-activated protein kinase. *Cell* **89,** 63–72
12. Yan, F., and Polk, D. B. (2001) Kinase suppressor of ras is necessary for tumor necrosis factor alpha activation of extracellular signal-regulated kinase/mitogen-activated protein kinase in intestinal epithelial cells. *Cancer Res.* **61,** 963–969
13. Brennan, D. F., Dar, A. C., Hertz, N. T., Chao, W. C., Burlingame, A. L., Shokat, K. M., and Barford, D. (2011) A Raf-induced allosteric transition of KSR stimulates phosphorylation of MEK. *Nature* **472,** 366–369
14. Kamps, M. P., and Sefton, B. M. (1986) Neither arginine nor histidine can carry out the function of lysine-295 in the ATP-binding site of p60src. *Mol. Cell. Biol.* **6,** 751–757
15. Roy, F., Laberge, G., Douziech, M., Ferland-McCollough, D., and Therrien, M. (2002) KSR is a scaffold required for activation of the ERK/MAPK module. *Genes Dev.* **16,** 427–438
16. Nguyen, A., Burack, W. R., Stock, J. L., Kortum, R., Chaika, O. V., Afkarian, M., Muller, W. J., Murphy, K. M., Morrison, D. K., Lewis, R. E., McNeish, J., and Shaw, A. S. (2002) Kinase suppressor of Ras (KSR) is a scaffold which facilitates mitogen-activated protein kinase activation *in vivo*. *Mol. Cell. Biol.* **22,** 3035–3045
17. Cacace, A. M., Michaud, N. R., Therrien, M., Mathes, K., Copeland, T., Rubin, G. M., and Morrison, D. K. (1999) Identification of constitutive and ras-inducible phosphorylation sites of KSR. Implications for 14-3-3 binding, mitogen-activated protein kinase binding, and KSR overexpression. *Mol. Cell. Biol.* **19,** 229–240
18. Therrien, M., Michaud, N. R., Rubin, G. M., and Morrison, D. K. (1996) KSR modulates signal propagation within the MAPK cascade. *Genes Dev.* **10,** 2684–2695
19. Jacobs, D., Glossip, D., Xing, H., Muslin, A. J., and Kornfeld, K. (1999) Multiple docking sites on substrate proteins form a modular system that mediates recognition by ERK MAP kinase. *Genes Dev.* **13,** 163–175
20. Rajakulendran, T., Sahmi, M., Lefrançois, M., Sicheri, F., and Therrien, M. (2009) A dimerization-dependent mechanism drives RAF catalytic activation. *Nature* **461,** 542–545
21. Xing, H., Kornfeld, K., and Muslin, A. J. (1997) The protein kinase KSR interacts with 14-3-3 protein and Raf. *Curr. Biol.* **7,** 294–300
22. Bell, B., Xing, H., Yan, K., Gautam, N., and Muslin, A. J. (1999) KSR-1 binds to G-protein $\beta\gamma$ subunits and inhibits beta gamma-induced mitogen-activated protein kinase activation. *J. Biol. Chem.* **274,** 7982–7986
23. Smith, F. D., Langeberg, L. K., Cellurale, C., Pawson, T., Morrison, D. K., Davis, R. J., and Scott, J. D. (2010) AKAP-Lbc enhances cyclic AMP control of the ERK1/2 cascade. *Nat. Cell Biol.* **12,** 1242–1249
24. Müller, J., Ory, S., Copeland, T., Piwnica-Worms, H., and Morrison, D. K. (2001) C-TAK1 regulates Ras signaling by phosphorylating the MAPK scaffold, KSR1. *Mol. Cell* **8,** 983–993
25. Ory, S., Zhou, M., Conrads, T. P., Veenstra, T. D., and Morrison, D. K. (2003) Protein phosphatase 2A positively regulates Ras signaling by dephosphorylating KSR1 and Raf-1 on critical 14-3-3 binding sites. *Curr. Biol.* **13,** 1356–1364
26. McKay, M. M., Ritt, D. A., and Morrison, D. K. (2009) Signaling dynamics of the KSR1 scaffold complex. *Proc. Natl. Acad. Sci. U.S.A.* **106,** 11022–11027
27. McKay, M. M., and Morrison, D. K. (2007) Caspase-dependent cleavage disrupts the ERK cascade scaffolding function of KSR1. *J. Biol. Chem.* **282,** 26225–26234
28. Qiao, Y., Molina, H., Pandey, A., Zhang, J., and Cole, P. A. (2006) Chemical rescue of a mutant enzyme in living cells. *Science* **311,** 1293–1297
29. Biscardi, J. S., Maa, M. C., Tice, D. A., Cox, M. E., Leu, T. H., and Parsons, S. J. (1999) c-Src-mediated phosphorylation of the epidermal growth factor receptor on Tyr^{845} and Tyr^{1101} is associated with modulation of receptor function. *J. Biol. Chem.* **274,** 8335–8343
30. Amrein, K. E., Panholzer, B., Molnos, J., Flint, N. A., Scheffler, J., Lahm, H. W., Bannwarth, W., and Burn, P. (1994) Mapping of the p56^{lck}-mediated phosphorylation of GAP and analysis of its influence on p21ras-GTPase activity in vitro. *Biochim. Biophys. Acta* **1222,** 441–446
31. Park, S., Liu, X., Pawson, T., and Jove, R. (1992) Activated Src tyrosine kinase phosphorylates Tyr-457 of bovine GTPase-activating protein (GAP) in vitro and the corresponding residue of rat GAP *in vivo*. *J. Biol. Chem.* **267,** 17194–17200
32. Fabian, J. R., Daar, I. O., and Morrison, D. K. (1993) Critical tyrosine residues regulate the enzymatic and biological activity of Raf-1 kinase. *Mol. Cell. Biol.* **13,** 7170–7179
33. Marais, R., Light, Y., Paterson, H. F., Mason, C. S., and Marshall, C. J. (1997) Differential regulation of Raf-1, A-Raf, and B-Raf by oncogenic ras and tyrosine kinases. *J. Biol. Chem.* **272,** 4378–4383
34. Diaz, B., Barnard, D., Filson, A., MacDonald, S., King, A., and Marshall, M.

(1997) Phosphorylation of Raf-1 serine 338-serine 339 is an essential regulatory event for Ras-dependent activation and biological signaling. *Mol. Cell. Biol.* **17,** 4509–4516
35. Klinghoffer, R. A., Sachsenmaier, C., Cooper, J. A., and Soriano, P. (1999) Src family kinases are required for integrin but not PDGFR signal transduction. *EMBO J.* **18,** 2459–2471
36. Winkler, C., Denker, K., Wortelkamp, S., and Sickmann, A. (2007) Silver- and Coomassie-staining protocols. Detection limits and compatibility with ESI MS. *Electrophoresis* **28,** 2095–2099
37. Burkhart, J. M., Schumbrutzki, C., Wortelkamp, S., Sickmann, A., and Zahedi, R. P. (2012) Systematic and quantitative comparison of digest efficiency and specificity reveals the impact of trypsin quality on MS-based proteomics. *J. Proteomics* **75,** 1454–1462
38. Beck, F., Lewandrowski, U., Wiltfang, M., Feldmann, I., Geiger, J., Sickmann, A., and Zahedi, R. P. (2011) The good, the bad, the ugly. Validating the mass spectrometric analysis of modified peptides. *Proteomics* **11,** 1099–1109
39. Burkhart, J. M., Premsler, T., and Sickmann, A. (2011) Quality control of nano-LC-MS systems using stable isotope-coded peptides. *Proteomics* **11,** 1049–1057
40. Olsen, J. V., de Godoy, L. M., Li, G., Macek, B., Mortensen, P., Pesch, R., Makarov, A., Lange, O., Horning, S., and Mann, M. (2005) Parts per million mass accuracy on an Orbitrap mass spectrometer via lock mass injection into a C-trap. *Mol. Cell. Proteomics* **4,** 2010–2021
41. Kessner, D., Chambers, M., Burke, R., Agus, D., and Mallick, P. (2008) ProteoWizard. Open source software for rapid proteomics tools development. *Bioinformatics* **24,** 2534–2536
42. Vaudel, M., Barsnes, H., Berven, F. S., Sickmann, A., and Martens, L. (2011) SearchGUI. An open-source graphical user interface for simultaneous OMSSA and X!Tandem searches. *Proteomics* **11,** 996–999
43. Vaudel, M., Breiter, D., Beck, F., Rahnenführer, J., Martens, L., and Zahedi, R. P. (2013) D-score. A search engine independent MD-score. *Proteomics* **13,** 1036–1041
44. Xia, F., Li, J., Hickey, G. W., Tsurumi, A., Larson, K., Guo, D., Yan, S.-J., Silver-Morse, L., and Li, W. X. (2008) Raf activation is regulated by tyrosine 510 phosphorylation in Drosophila. *PLoS Biol.* **6,** e128
45. Kortum, R. L., and Lewis, R. E. (2004) The molecular scaffold KSR1 regulates the proliferative and oncogenic potential of cells. *Mol. Cell. Biol.* **24,** 4407–4416
46. Dougherty, D. A. (2007) Cation-π interactions involving aromatic amino acids. *J. Nutr.* **137,** 1504S–1508S
47. Jiménez, J. L., Hegemann, B., Hutchins, J. R., Peters, J.-M., and Durbin, R. (2007) A systematic comparative and structural analysis of protein phosphorylation sites based on the mtcPTM database. *Genome Biol.* **8,** R90
48. Hanks, S. K., and Hunter, T. (1995) Protein kinases 6. The eukaryotic protein kinase superfamily. Kinase (catalytic) domain structure and classification. *FASEB J.* **9,** 576–596
49. Goettel, J. A., Liang, D., Hilliard, V. C., Edelblum, K. L., Broadus, M. R., Gould, K. L., Hanks, S. K., and Polk, D. B. (2011) KSR1 is a functional protein kinase capable of serine autophosphorylation and direct phosphorylation of MEK1. *Exp. Cell Res.* **317,** 452–463
50. Abe, M. K., Kahle, K. T., Saelzler, M. P., Orth, K., Dixon, J. E., and Rosner, M. R. (2001) ERK7 is an autoactivated member of the MAPK family. *J. Biol. Chem.* **276,** 21272–21279
51. Cole, A., Frame, S., and Cohen, P. (2004) Further evidence that the tyrosine phosphorylation of glycogen synthase kinase-3 (GSK3) in mammalian cells is an autophosphorylation event. *Biochem. J.* **377,** 249–255
52. Lochhead, P. A., Sibbet, G., Morrice, N., and Cleghon, V. (2005) Activation-loop autophosphorylation is mediated by a novel transitional intermediate form of DYRKs. *Cell* **121,** 925–936
53. Cabeza-Arvelaiz, Y., and Schiestl, R. H. (2012) Transcriptome analysis of a rotenone model of parkinsonism reveals complex I-tied and -untied toxicity mechanisms common to neurodegenerative diseases. *PLoS One* **7,** e44700
54. Baljuls, A., Mueller, T., Drexler, H. C., Hekman, M., and Rapp, U. R. (2007) Unique N-region determines low basal activity and limited inducibility of A-RAF kinase. The role of N-region in the evolutionary divergence of RAF kinase function in vertebrates. *J. Biol. Chem.* **282,** 26575–26590
55. Kilkenny, D. M., Rocheleau, J. V., Price, J., Reich, M. B., and Miller, G. G. (2003) c-Src regulation of fibroblast growth factor-induced proliferation in murine embryonic fibroblasts. *J. Biol. Chem.* **278,** 17448–17454
56. Sugimoto, T., Stewart, S., Han, M., and Guan, K. L. (1998) The kinase suppressor of Ras (KSR) modulates growth factor and Ras signaling by uncoupling Elk-1 phosphorylation from MAP kinase activation. *EMBO J.* **17,** 1717–1727
57. Lin, J., Harding, A., Giurisato, E., and Shaw, A. S. (2009) KSR1 modulates the sensitivity of mitogen-activated protein kinase pathway activation in T cells without altering fundamental system outputs. *Mol. Cell. Biol.* **29,** 2082–2091